Cell Therapy with Embryonic Stem Cell-Derived Cardiomyocytes Encapsulated in Injectable Nanomatrix Gel Enhances Cell Engraftment and Promotes Cardiac Repair

Kiwon Ban,[†,⊥] Hun-Jun Park,[†,‡,⊥] Sangsung Kim,[†] Adinarayana Andukuri,[†] Kyu-Won Cho,[†] Jung Wook Hwang,[†] Ho Jin Cha,[†] Sang Yoon Kim,[†] Woan-Sang Kim,[†] Ho-Wook Jun,[§] and Young-Sup Yoon*[,†]

[†]Department of Medicine, Division of Cardiology, Emory University School of Medicine, Atlanta, Georgia 30322, United States, [‡]Division of Cardiology, Department of Internal Medicine, Seoul St. Mary's Hospital, The Catholic University of Korea, Seoul, Republic of Korea, and [§]Department of Biomedical Engineering, University of Alabama at Birmingham, Birmingham, Alabama 35203, United States. [⊥]K. Ban and H.-J. Park have contributed equally to this report.

ABSTRACT A significant barrier to the therapeutic use of stem cells is poor cell retention *in vivo*. Here, we evaluate the therapeutic potential and long-term engraftment of cardiomyocytes (CMs) derived from mouse embryonic stem cells (mESCs) encapsulated in an injectable nanomatrix gel consisting of peptide amphiphiles incorporating cell adhesive ligand Arg-Gly-Asp-Ser (PA-RGDS) in experimental myocardial infarction (MI). We cultured rat neonatal CMs in PA-RGDS for 7 days and found that more than 90% of the CMs survived. Next, we intramyocardially injected mouse CM cell line HL-1 CMs with or without PA-RGDS into uninjured hearts. Histologic examination and flow cytometry analysis of digested heart tissues showed approximately 3-fold higher engraftment in the mice that received CMs with PA-RGDS compared to those without PA-RGDS. We further investigated the therapeutic effects and long-term engraftment of mESC-CMs with PA-RGDS on MI in comparison with PBS control, CM-only, and PA-RGDS only. Echocardiography demonstrated that the CM-only and CM+PA-RGDS groups showed higher cardiac function at week 2 compared to other groups. However, from 3 weeks, higher cardiac function was maintained only in the CM+PA-RGDS group; this was sustained for 12 weeks. Confocal microscopic examination of the cardiac tissues harvested at 14 weeks demonstrated sustained engraftment and integration of mESC-CMs into host myocardium in the CM+PA-RGDS group only. This study for the first time demonstrated that PA-RGDS encapsulation can enhance survival of mESC-derived CMs and improve cardiac function post-MI. This nanomatrix gel-mediated stem cell therapy can be a promising option for treating MI.

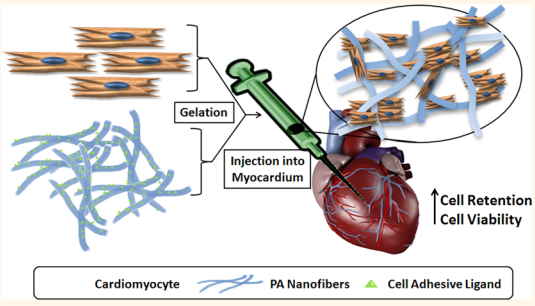

KEYWORDS: PA-RGDS · myocardial infarction · pluripotent stem cell · cardiomyocyte · cardiac regeneration

Heart disease is one of the leading causes of death in the United States, accounting for more than 600 000 deaths per year, with the majority of fatalities due to coronary artery disease and correlating heart failure.[1] Due to limited therapeutic options for severe MI and advanced heart failure, cell-based therapy has emerged as a promising therapeutic option.[2] Particularly, cardiomyocytes (CMs) derived from pluripotent stem cells (PSCs) including both embryonic stem cells (ESCs) and the recently identified induced pluripotent stem cells (iPSCs)[3,4] are regarded as one of the most promising sources for cardiac repair.[5] CMs differentiated from PSCs have unquestioned cardiomyogenic potential,[6] in contrast to various adult stem cells, of which the capacity to differentiate into significant numbers of definitive CMs is controversial.[7] PSC-derived CMs have a clear cardiac phenotype, cardiac-type electrophysiologic characteristics, and expression of expected genes and proteins.[8] Several recent studies have shown that transplantation of PSC-derived CMs into rodent infarct models helped preserve cardiac function.[9]

* Address correspondence to yyoon5@emory.edu.

Received for review August 18, 2014 and accepted September 11, 2014.

Published online September 11, 2014
10.1021/nn504617g

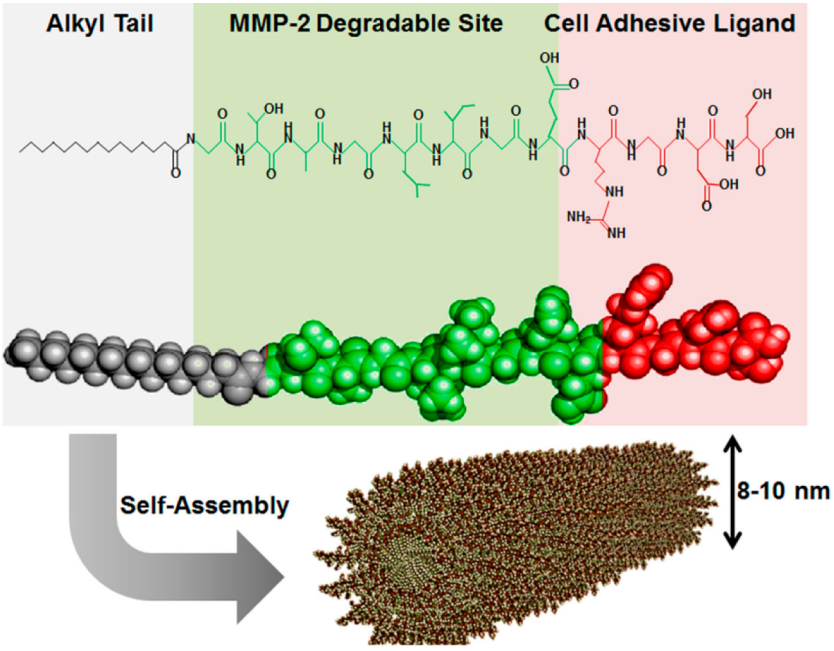

Figure 1. Structure of PA-RGDS.

However, it is now widely recognized that retention of CMs delivered into heart is surprisingly low. The survival rate is only 50% immediately after injection and drops to 10% in as little as 1 week.[10] The longest reported survival of human PSC-derived CMs after direct injection into murine myocardium did not exceed 12 weeks.[11] These issues have necessitated the development of biomaterial-based strategies in which extracellular matrix (ECM)-mimicking biomaterials can promote cell survival, maturation, and integration with the host myocardium by providing a nurturing environment with the necessary factors, frequently lacking in the infarcted heart.[12] Recent developments in nanoscale design allow us to tailor biomaterials to very closely mimic the ECM, which can provide the cells with a protective microenvironment while simultaneously promoting localized ECM formation and intercellular connections.

Accordingly, we aimed to develop a novel strategy to enhance the therapeutic effects of PSC-derived CMs by using self-assembled biodegradable peptide amphiphile (PA) nanomatrices. PAs are a class of self-assembling peptides that combine a short hydrophobic sequence with a hydrophilic, bioactive peptide sequence, presenting a promising approach to achieve this goal (Figure 1).[13] For this study, we generated PA-RGDS, an ECM-mimicking injectable nanomatrix, by incorporating cell adhesive ligand Arg-Gly-Asp-Ser (RGDS) and matrix metalloprotease-2 (MMP-2) degradable sequence Gly-Thr-Ala-Gly-Leu-Ile-Gly-Gln (GTAGLIGQ) into the PA.[14] The amphiphilicity of this PA allows self-assembly into three-dimensional (3D) networks of high aspect ratio nanofibers similar to ECM protein nanofibers under physiological conditions. In addition, RGDS, a fibronectin-derived cell adhesive ligand, is incorporated into PA to promote cell adhesion and survival, and its favorable effect has been extensively confirmed by a variety of cell types such as human mesenchymal stem cells, human umbilical vein endothelial cells, aortic smooth muscle cells, and pancreatic beta cells.[15−28] Lastly, incorporation of MMP-2 degradable sequences into PAs is expected to allow progressive degradation of the scaffold and replacement by natural ECM produced by the cells, as the heart tissue displays increased MMP production under ischemic conditions.[29−31] It also enhances the migration of encapsulated CMs into the host myocardium. These PA-RGDS closely mimic the physical as well as the biochemical complexity of the native ECM.

Hence, we hypothesized that encapsulation of mESC-derived CMs with injectable PA-RGDS nanomatrix gel would improve cardiac function post-MI through increased cell survival and retention within the host myocardium. Subsequently, we found that this PA-RGDS nanomatrix enabled long-term survival of mESC-CMs in ischemic hearts and their integration into host myocardium and promoted cardiac repair following experimental MI.

RESULTS

PA-RGDS Is Not Cytotoxic to Cardiomyocytes. To examine the cytotoxicity of PA-RGDS to CMs, neonatal rat cardiomyocytes (NRCMs) were embedded within PA-RGDS nanomatrix gel and cultured for 7 days under normal CM culture conditions, and Live/Dead staining was performed. As shown in Figure 2, the majority of NRCMs encapsulated with PA-RGDS were alive (green) after 7 days of culture, and less than one-tenth of cells

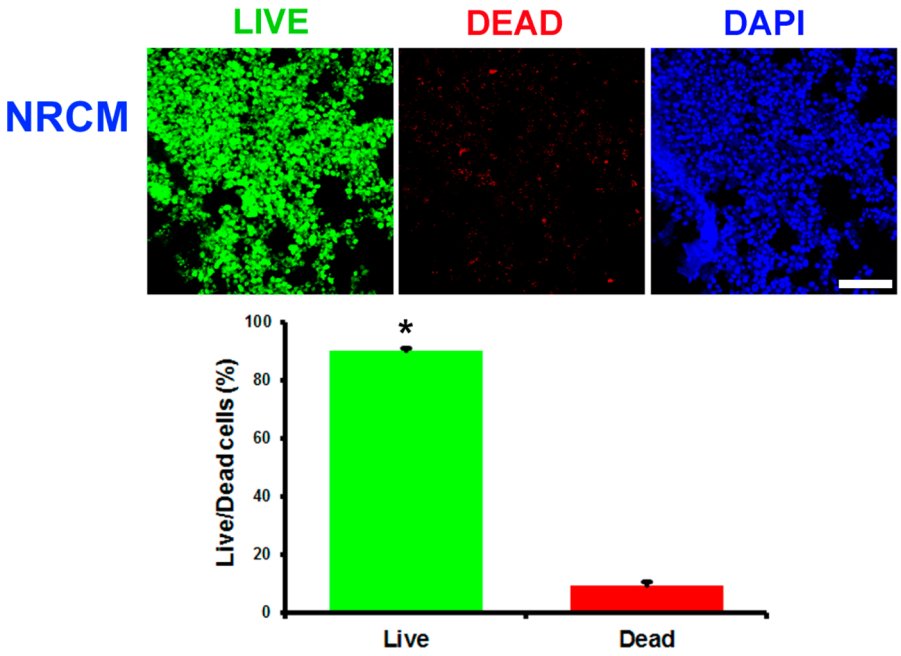

Figure 2. Evaluation of cellular behaviors of cardiomyocytes encapsulated in PA-RGDS. Representative Live/Dead assay images of NRCMs after 7 days of culture in normoxic conditions. Bar graph summarizes the results of the Live/Dead assay. *$p < 0.0001$; $N = 3$. Scale bars, 20 μm.

were dead (red). These data indicate that PA-RGDS gel supports the viability of CMs over a 7-day culture period (live *vs* dead: 90.7 ± 6.2% *vs* 9.3 ± 0.8%, $p < 0.001$) (Figure 2).

Cytoprotective Effects of PA-RGDS Encapsulation against Oxidative Stress. Since a main cause of poor survival of transplanted cells in the ischemic heart is oxidative stress,[12] we investigated whether encapsulation of the CMs with PA-RGDS could increase their survival when exposed to H_2O_2, which simulates ischemic conditions *in vitro*. As shown in Figure 3A, the results from live/dead staining demonstrated that encapsulation of NRCMs with PA-RGDS significantly improved viability compared to NRCMs without encapsulation ($p < 0.001$) (Figure 3A). Concordantly, CM/PA-RGDS constructs exposed to H_2O_2 released significantly less LDH compared to bare NRCMs ($p < 0.001$) (Figure 3B). These results indicate that encapsulating the CMs with PA-RGDS can promote CM survival under conditions of oxidative stress.

***In Vivo* Degradation Kinetics of PA-RGDS.** To examine the *in vivo* degradation behavior of the PA-RGDS, PA-RGDS that was prelabeled with CM-DiI, a red fluorescent dye (Supplementary Figure 1A), was allowed to self-assemble into a three-dimensional gel. The gels were then intramyocardially injected into the hearts of C57B6 mice, after myocardial infarction (MI) was induced by ligation of the left anterior descending coronary artery.[32,33] The mice were then euthanized at 1, 2, 4, and 6 weeks after injections ($N = 3$ per time point), and the hearts were harvested. Through histological evaluation under confocal microscopy, we found that the amount of red fluorescent PA-RGDS was gradually reduced in heart sections over time and was almost degraded in all three hearts by 6 weeks (Supplementary Figure 1B).

PA-RGDS Increased Retention of Transplanted Cardiomyocytes in Intact Heart. To investigate the effects of PA-RGDS on CM engraftment and survival *in vivo*, we prelabeled cultured HL-1 CMs,[34] an immortalized mouse CM cell line, with CM-DiI and injected them into the intact hearts of athymic nude mice (2×10^5 cells per mouse) in the absence or presence of PA-RGDS. After sacrificing mice at 1 week, we performed immunostaining and flow cytometry. Confocal microscopic examination demonstrated that the number of engrafted CMs was substantially higher in the PA-RGDS-encapsulated HL-1 CM group than in the bare HL-1 CM group (Figure 4A). For more accurate quantification of these engrafted/surviving cells, we performed flow cytometry analysis of enzymatically digested heart tissues (Figure 4B).[35] We found that the retention rate of HL-1 CMs was approximately 3-fold higher when encapsulated with PA-RGDS than without encapsulation. Immunohistochemistry further showed that the injected CMs in PA-RGDS integrated well within host myocardium and maintained expression of cardiac-specific protein ACTN2 (or α-sarcomeric actinin). These results suggest that encapsulation with PA-RGDS significantly increased the retention and integration of the injected CMs into the heart *in vivo* (Figure 4C).

Generation and Purification of Cardiomyocytes from Mouse Embryonic Stem Cells. To generate CMs, undifferentiated mouse ESCs (J1) were induced to form EBs. Day-4 EBs were replated as monolayers in the presence of ascorbic acid (Supplementary Figure 2A).[32] Spontaneously beating clumps began to appear 3–4 days later

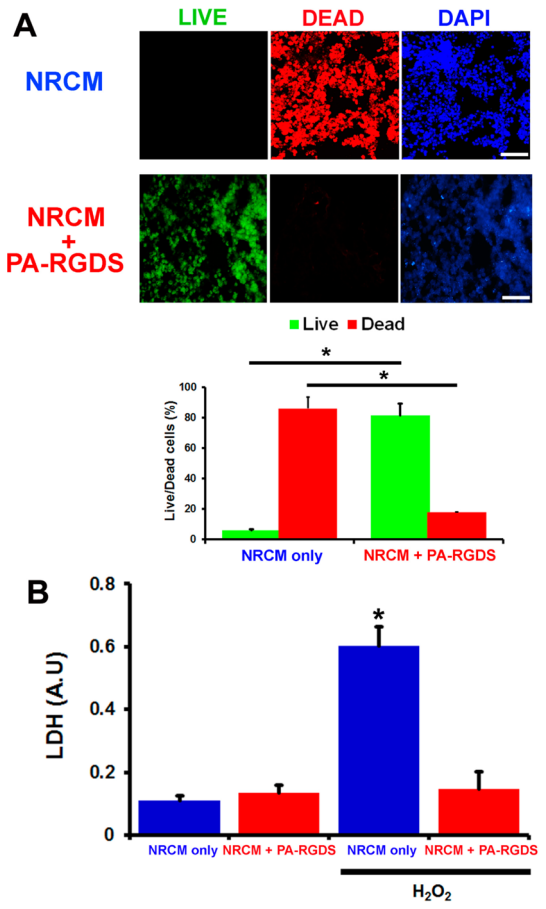

Figure 3. Cytoprotective effects of PA-RGDS encapsulation against H_2O_2. (A) Encapsulation of NRCMs with PA-RGDS increased cell survival after H_2O_2 (200 μM) treatment as determined by the Live/Dead assay. *$p < 0.001$ compared with CM only group; $N = 3$. Scale bars, 20 μm. (B) Cell viability was also measured by extracellular release of LDH. *$p < 0.001$ compared with H_2O_2-untreated controls.

(Supplementary Movie 1). A prior study demonstrated that CMs can be purified from differentiating PSCs by the addition of lactate to glucose-depleted medium, due to the metabolic differences between CMs and non-CMs.[36] Therefore, at 7 days, we replaced the culture medium with glucose-depleted medium supplemented with 1 mM lactate, and the cells were cultured for another 7 days. Flow cytometry analysis showed that the percentage of cardiac troponin T (TNNT2)-positive cells was increased from 48.5 ± 5.1% at day 11 (before lactate treatment) to 77.2 ± 6.8% at day 18 (Supplementary Figure 2B). Immunocytochemistry further demonstrated that a majority of differentiated mESCs expressed CM-specific proteins ACTN2, TNNT2, and MYH6/7 (or α/β MHC), confirming their CM nature (Supplementary Figure 2C–E). Collectively, these results indicate that our new differentiation system can successfully generate enriched CMs from mESCs.

CM/PA-RGDS Improved Cardiac Function and Reduced Scar Formation after MI. Next, we investigated the therapeutic effects of these enriched mESC-CMs encapsulated with PA-RGDS on MI. After the mice were randomized to four groups, each group received the following materials directly into the periinfarct region immediately after MI: mESC-CMs encapsulated with PA-RGDS, mESC-CMs only, PA-RGDS only, and phosphate-buffered saline (PBS) control. Cells were prelabeled with CM-DiI before cell injection for tracking in histological sections. Echocardiography was performed weekly for 4 weeks (Figure 5A). One week post-MI, fractional shortening (FS) and ejection fraction (EF) did not differ significantly among the groups. At week 2, EF and FS were higher in the mESC-CM only and mESC-CM+PA-RGDS groups compared to the PA-RGDS only and PBS groups, although the differences did not reach statistical significance. From 3 weeks, the EF and FS were continuously increased in the mESC-CM+PA-RGDS group, while reduced in the mESC-CM only group and showed a significant difference between the mESC-CM+PA-RGDS group compared to the other three groups at 4 weeks (Figure 5A). Masson's trichrome staining of the cardiac tissue harvested at 4 weeks demonstrated that the mESC-CM+PA-RGDS group showed significantly reduced fibrosis compared to the other three groups ($p < 0.05$) (Figure 5B).

Fluorescent microscopic examination of the heart sections harvested at 4 weeks showed that the number of engrafted DiI-positive mESC-CMs was significantly higher in the mice receiving CMs encapsulated with PA-RGDS compared to those receiving only mESC-CMs (Figure 5C). Immunohistochemistry with MHC6/7 antibody further demonstrated that the injected CMs encapsulated with PA-RGDS were robustly engrafted and integrated into the host myocardium, forming clusters, and expressed representative CM proteins (Figure 5D).

Sustained Therapeutic Effects of mESC-CMs with PA-RGDS. Prior studies reported that the beneficial effects of ESCs were substantially diminished by 3–4 weeks, mostly due to massive cell death or ejection from the myocardium.[11] Hence, we monitored the long-term therapeutic effects of the mESC-CM+PA-RGDS-treated group in comparison to the CM-only injected group over 12 weeks (Figure 6A). Echocardiography showed that both EF and FS were slightly decreased until 8 weeks but were maintained during the rest of the follow-up in the mESC-CM+PA-RGDS group, while the indices were progressively decreased in the mESC-CM-only group (Figure 6A). We further examined the characteristics of engrafted mESC-CMs in histologic sections of the harvested hearts at 14 weeks. Microscopic examination after DAPI counterstaining showed that a substantial number of DiI-labeled CMs were still visible in the heart tissues that received mESC-CMs with PA-RGDS, while DiI-labeled CMs were hardly seen in the mESC-CM-only group (Figure 6B). Immunostaining for MYH6/7 demonstrated that these engrafted CMs were well integrated into the host myocardium, and concomitant staining with Gja1 further showed

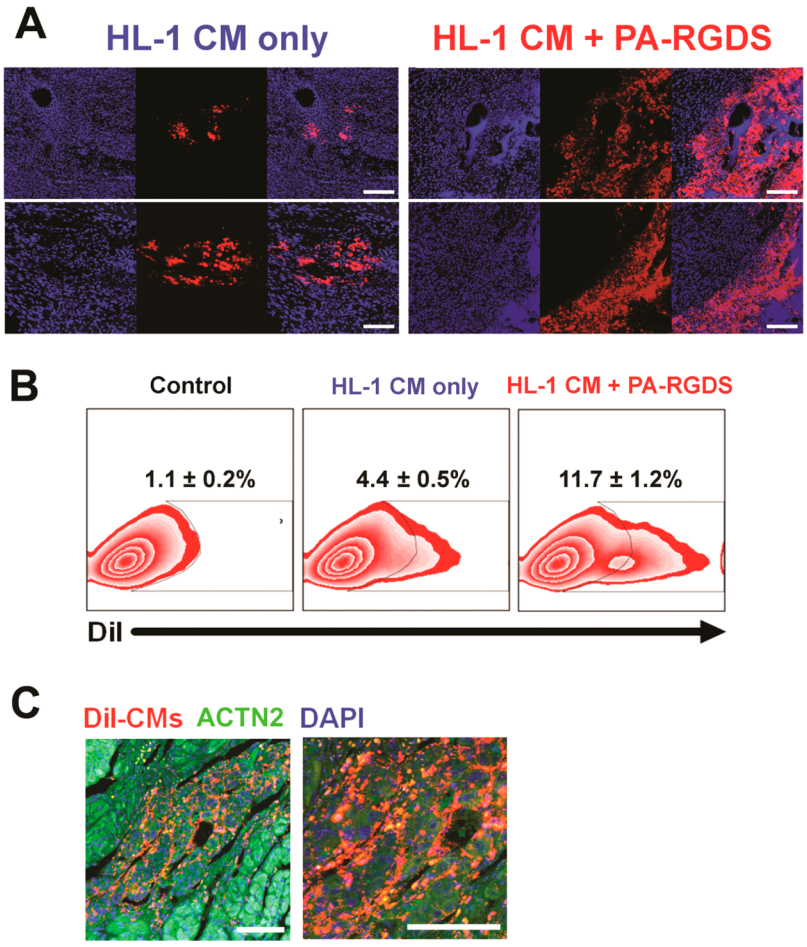

Figure 4. Survival and engraftment of HL-1 CMs after injection into uninjured mouse hearts. Seven days after injection of dilabeled (red) HL-1 CMs encapsulated with or without PA-RGDS into intact mouse hearts, mice were sacrificed and hearts were collected. (A) Confocal microscopic images of sectioned heart tissue after DAPI staining. DiI: red fluorescence. DAPI: blue fluorescence. Scale bars, 200 μm. (B) Quantification of engrafted HL-1 CMs by flow cytometry following cardiac tissue digestion into cell suspension; $N = 3$. (C) Confocal microscopic images of sectioned heart tissues after staining with ACTN2 in the mice receiving HL-1 CMs encapsulated with PA-RGDS. Green: ACTN2 staining. Scale bars, 20 μm.

formation of gap junctions between the engrafted CMs and host CMs (Figure 6D). Together, these data suggest that myocardial injection of mESC-CMs encapsulated with PA-RGDS markedly enhanced cell retention within the injured myocardium, induced integration of mESC-CMs with host myocardium, and sustained therapeutic effects over several months.

DISCUSSION

The potential success of stem cell-based therapy for cardiac regeneration has been consistently hindered by a critical inability to retain implanted cells in heart.[37] In most stem cell studies, myocardially injected cells have a very low survival rate.[38] Thus, various natural and artificial biomaterials have been assessed for cardiac repair with adult or pluripotent stem cells.[12,38−40] Among them, PA-based materials have emerged as a promising option due to rapid gel-like 3D network formation, ECM-like nanostructures, modular designs, and biodegradability. Although PA-based biomaterials were used for cell delivery of bone marrow-derived cells, there have not been any studies that explored their effects on pluripotent stem cell-derived CMs and their long-term fate.[41]

The present study shows that PA-RGDS is able to enhance cell retention and improves cardiac function. While the cardiac function of the mESC-CM-only injected group was improved to a similar extent to the mESC-CMs encapsulated with PA-RGDS group by 2 weeks after treatment, suggesting regenerative effects of bare mESC-CMs at an early phase, such effects disappeared after 3 weeks. Histologic examination clearly demonstrated that the mESC-CM-only injected group showed virtually complete disappearance of the injected cells over 14 weeks. However, the PA-RGDS-encapsulated mESC-CM group showed long-term cellular engraftment and integration into host myocardium, expressed mature and structural CM proteins such as cTNT and MHC6/7, formed gap junctions with host CMs, and maintained improved cardiac function, indicating the effectiveness of PA-RGDS on the function of injected mESC-CMs. These results indicate that

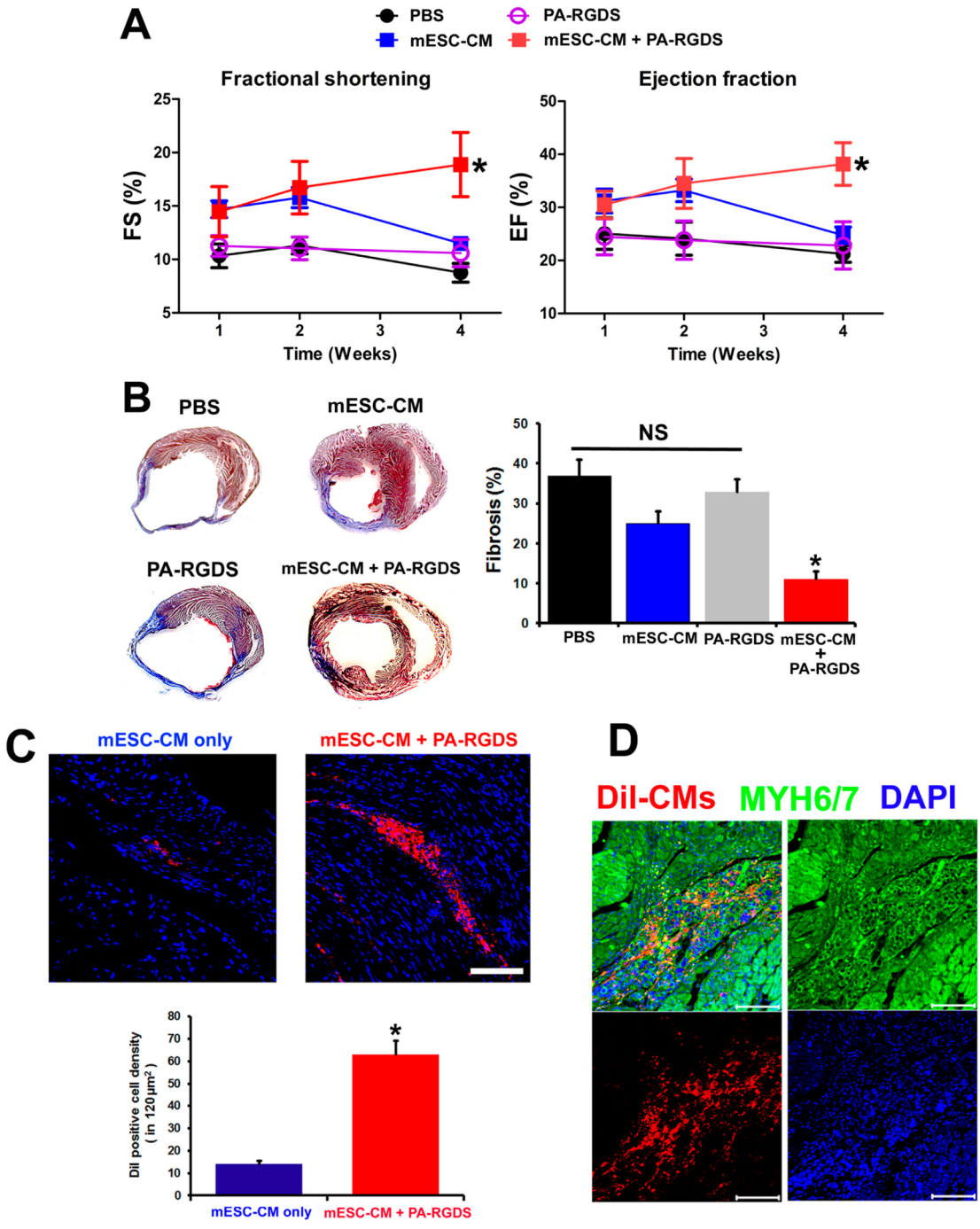

Figure 5. Favorable effects of mESC-CMs with PA-RGDS on mouse experimental MI. (A) Improvement of cardiac function in mice receiving mESC-derived CMs with PA-RGDS. Fractional shortening (FS: left) and ejection fraction (EF: right) were significantly higher in the mESC-CM+PA-RGDS group compared to the three other groups measured by echocardiography. Repeated-measures ANOVA was used for statistical analyses. *$p < 0.05$; $N = 6–10$ per group. (B) Representative images from the four treated groups showing cardiac fibrosis after staining with Masson's trichrome in the hearts harvested 4 weeks after MI and their quantification results. *$p < 0.05$; $N = 6$. (C) Confocal microscopic images of heart sections collected 4 weeks after MI and cell injection showed that the engraftment of Dil-labeled mESC-CMs was substantially higher when cells were encapsulated. *$p < 0.05$; $N = 3$. (D) The Dil-mESC-CMs (red fluorescence) expressed MYH6/7 (green) and were well integrated into host myocardium. Scale bars, 20 μm.

even though the gels may degrade by week 6, the cells delivered by the gels show significant long-term favorable outcomes. From this, we may infer that PA-RGDS indeed provides the cells with a protective environment during the early stage of implantation, which is critical for cell engraftment and survival, leading to improved retention and eventual interactions with host tissue.

This study is the first to investigate the therapeutic effects of CMs derived from PSCs in combination with

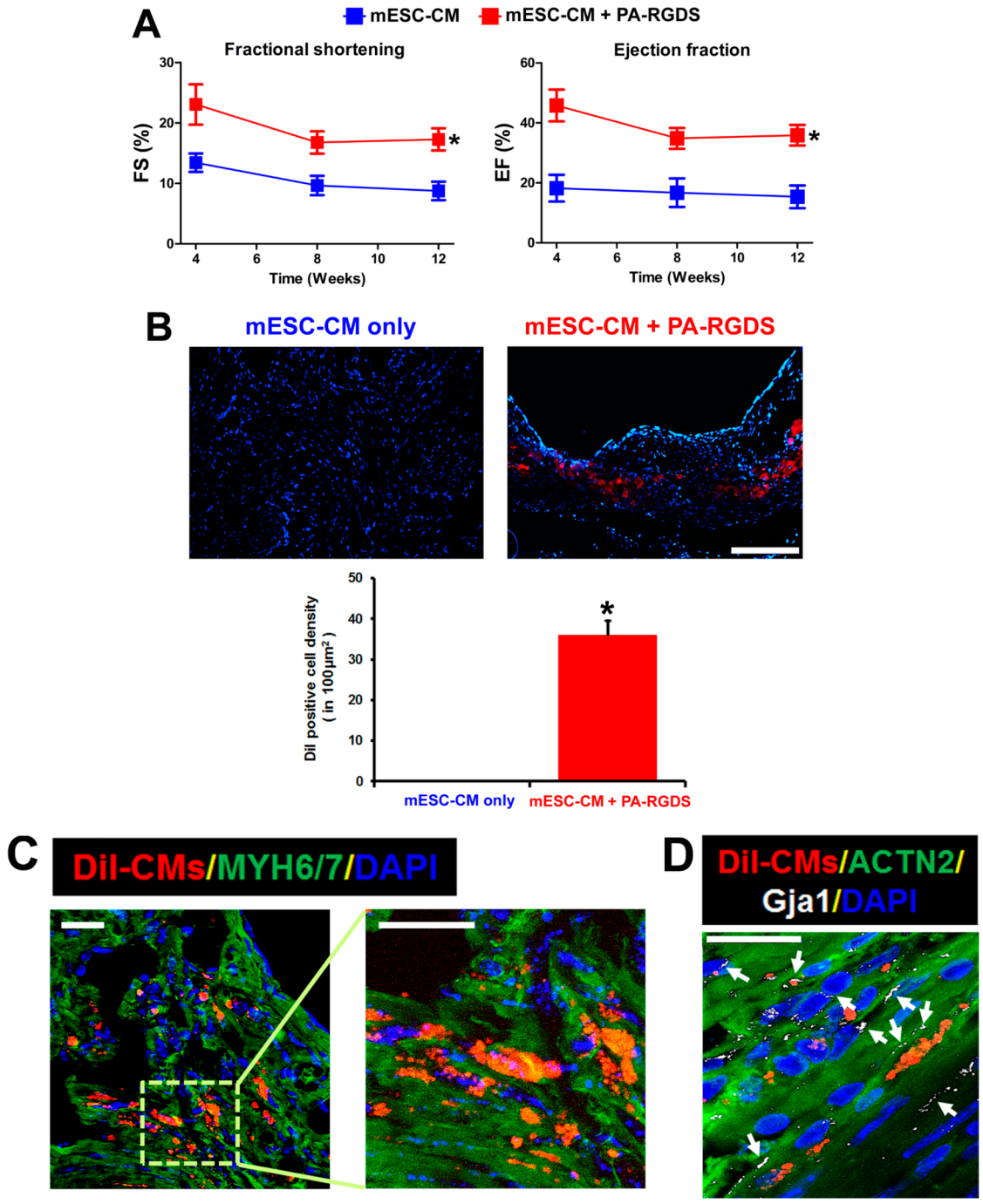

Figure 6. Sustained therapeutic effects of mESC-CMs with PA-RGDS on a mouse model of MI. (A) EF and FS measured by echocardiography were significantly greater in the mESC-CM+PA-RGDS group compared to the mESC-CM-only injected group. Repeated-measures ANOVA was used for statistical analyses. *$p < 0.05$. $N = 6$ per group. (B) Representative confocal microscopic images showing engraftment of DiI-labeled mESC-CMs in hearts harvested at 14 weeks compared to the CM-only injected group and the CMs with PA-RGDS group and their quantification (lower panel) *$p < 0.05$. $N = 5$. (C, D) Confocal microscopic images show integration of implanted mESC-CMs (DiI, red fluorescence) into ischemic myocardium, as evidenced by expression of Myh6/7 (C, green), Actn2 (D, green), and Gja1 (D, white). Hearts harvested from the mESC-CM+PA-RGDS group at 14 weeks. Scale bars, 20 μm.

injectable PA-RGDS nanomatrix gel. While there have been numerous studies examining the effects of biomaterial-mediated cell therapy for cardiac regeneration, most studies employed adult stem cells such as mesenchymal stem cells and endothelial progenitor cells. However, the trans-differentiation potential of those cells into CMs is limited and their underlying mechanism is paracrine or humoral effects on surviving myocardium.[42] Ideally, it would be better to generate new myocardial tissues in hearts by providing new CMs. Here, our strategy was to meet this end by combining PSC-derived CMs, which have the clearest

potential for generating new CMs in injured hearts,[2] with PA-RGDS, which has the potential to address low cell survival.

The PA-RGDS used in this study was designed to provide a protective microenvironment for CMs *in vivo* by incorporating PAs with RGDS cell adhesive ligands, MMP-2 degradation sites, and self-assembly into three-dimensional nanofiber networks. The rapid polymerization kinetics of the PA-RGDS allows effective entrapment of mESC-derived CMs at the site of delivery, resulting in improved cell retention. The incorporation of RGDS cell adhesive ligand promotes the adhesion and retention of CMs inside the nanomatrix gel, especially since PSC-derived CMs have poor adhesion capacities. MMP-2 degradable sites play an important role in the slow integration of implanted CMs with host myocardium through their controlled degradation of the nanomatrix gel, as evidenced by the results of the degradation study. In addition, the 3D nanofiber network structure allows the transfer of nutrients and growth factors by diffusion, thereby promoting cell viability. Another important aspect of the PA-RGDS is the physical properties of the gels, which can be tuned to provide mechanical strength.[43] It has been previously assessed that the mechanical properties of PA-RGDS self-assembled under similar conditions determined by the storage modulus (G') have been observed to be around 100 Pa,[43] which puts them in the category of moderately stiff hydrogels with higher potential for cell encapsulation and delivery for soft tissue engineering applications such as cardiovascular tissues.[43] PA-RGDS nanomatrix gels were also observed to be structurally stable with well-defined cylindrical shape and increased durability for handling and transport. This is particularly important for early cell survival, as cardiac tissue scaffolds require enough mechanical strength to resist the cardiac cycle, but enough flexibility to allow the contractile function of implanted CMs. While the exact required mechanical stiffness to match native heart tissue remains unknown due to the vast changes in heart stiffness during diseased stages, the mechanical strength of PA-RGDS can be tuned for the application as previously reported.[43] Along with the biochemical cues provided by RGDS and the MMP-2 degradable sequences, this property may be important for initial retention and survival of implanted CMs.

CONCLUSION

This study demonstrates that PA-RGDS gel has the capacity to augment survival and integration of PSC-derived CMs, which leads to generation of new CMs over a few months and improves cardiac function. As it is biocompatible and already approved by FDA for clinical use, this injectable PA-RGDS-mediated pluripotent stem cell therapy can develop into a novel therapy for repairing injured hearts.

METHODS

Peptide Amphiphile Synthesis. Two peptide amphiphiles, C_{16}-GTAGLIGQRGDS (PA-RGDS) and C_{16}-GTAGLIGQS (PA-S), were synthesized *via* Fmoc-chemistry using an Aapptech Apex 396 peptide synthesizer as previously described.[23,27,28,43−45] The peptides were then alkylated at the N-termini *via* two 12 h reactions with palmitic acid and a mixture of *o*-benzotriazole-*N*,*N*,*N*′,*N*′-tetramethyluronium hexafluorophosphate and diisopropylethylamine dissolved in dimethylformamide. This was succeeded by cleavage from the resin and deprotection for 3 h, using a 40:1:1:1 cocktail of trifluoroacetic acid (TFA), deionized water, triisopropylsilane, and anisole. The collected samples were subjected to rotary evaporation to remove excess TFA, precipitated in ether, and lyophilized. Matrix-assisted laser desorption ionization time-of-flight (MALDI-TOF) mass spectrometry was utilized to confirm successful synthesis of PAs.

Self-Assembly of Peptide Amphiphile Gels. Stock solutions of PA-RGDS and PA-S [2% (weight/volume)] were individually prepared, and their respective pH was adjusted to 7 using sodium hydroxide (NaOH). The two PAs were then mixed in 1:1 molar ratio, and self-assembly into three-dimensional hydrogels was induced by combining 50 μL of PA solution with a mixture containing 15 μL of 0.1 M $CaCl_2$ and 25 μL of cell suspension. The molar ratio of PA and Ca^{2+} was held constant at 2.[27,43]

Isolation and Culture of Rat Neonatal Ventricular Cardiomyocytes. To isolate neonatal rat ventricular cardiomyocytes (NRCMs), the heart tissues from 3- to 5-day-old neonatal rats were carefully dissected and digested for 1−2 h with 50 U/mL collagenase type II (Worthington Biochemicals) in calcium- and bicarbonate-free Hanks' buffer with HEPES at room temperature, followed by overnight digestion with 0.5 mg/mL of trypsin (Invitrogen) at 4 °C. The number of noncardiac cells such as fibroblasts and endothelial cells was minimized by differential plating. A total of 2×10^6 isolated NRCMs were plated in a 100 mm dish and cultured at 37 °C in growth media containing Dulbecco's modified Eagle's medium/Ham's F-12 [1:1 (v/v); Invitrogen] supplemented with 10% fetal bovine serum (FBS) and 100 units/mL penicillin/streptomycin (Invitrogen). Following 24 h of culture, the medium was replaced by serum-free medium supplemented with 1% insulin-transferrin-selenium (ITS) in DMEM/F12 [1:1 (v/v)] for 24 h.[46]

Cultivation of HL-1 Cardiomyocytes. HL-1 CMs, a cell line derived from adult mouse atria, were received from Dr. William Claycomb (Louisiana State University, LA, USA) and cultivated as described in the literature.[34] The HL-1 CMs were plated in a dish coated with 12.5 μg/mL fibronectin (Sigma) and 0.02% gelatin (Sigma) and maintained in complete Claycomb medium (Sigma) supplemented with 10 μM norepinephrine (Sigma), 0.3 mM L-ascorbic acid (Sigma), 4 mM L-glutamine (Gibco), and 10% FBS (Sigma) in a 5% CO_2 atmosphere at 37 °C.

Evaluation of Cytotoxicity of PA-RGDS. In order to examine if PA-RGDS is cytotoxic to CMs, we performed Live/Dead staining (Invitrogen) for CMs cultured in PA-RGD gel. A total of 5×10^5 freshly isolated and cultured NRCMs contained in 50 μL of advanced DMEM media with 3% FBS were mixed with 50 μL of the PA-RGDS solution followed by the addition of 14 μL of $CaCl_2$ (0.1 M) solution to initiate gel polymerization. Subsequently, the CM/PA-RGDS constructs were cultured in CM culture medium containing advanced DMEM/F12 supplemented with 3% FBS and ITS for 7 days and harvested for Live/Dead staining. To show the live cell distribution, confocal images (z-stacks) were captured at either the center or the edge of CM/PA-RGDS constructs using a Zeiss LSM 510 Meta confocal laser scanning microscope and LSM 510 Image software (CLSM, Carl Zeiss). Quantification of live or dead cells was performed using ImageJ software.

Evaluation of *in Vivo* Biodegradation of PA-RGDS. To explore the nature of degradation of the PA-RGDS hydrogel *in vivo*, we

labeled PA-RGDS with CM-DiI, a red fluorescent dye, for tracking gels and intramyocardially injected it into the hearts of C57B6 mice where myocardial infarction was induced by ligation of the left anterior descending coronary artery. The mice were then euthanized 1, 2, 4, or 6 weeks after injections for histological evaluation ($N = 3$ per time point).

Assessment of Cytoprotective Effects of PA-RGDS on CMs against Oxidative Stress. To investigate whether encapsulation of CMs with PA-RGDS could provide cytoprotective effects against oxidative stress, we generated CM/PA-RGDS constructs by the method described above and cultured them in CM culture medium containing hydrogen peroxide (H_2O_2) (200 μM), simulating conditions of myocardial ischemia *in vitro*. Following 2 h exposure to hydrogen peroxide, CM/PA-RGDS constructs were harvested for Live/Dead staining. Culture medium was removed and subjected to lactase dehydrogenase (LDH) assay (LDH cytotoxicity assay kit, Sigma).[46] Briefly, 50 μL of culture medium was collected from cultured CM/PA-RGDS constructs (in triplicate) and transferred into a 96-well plate. After adding an equivalent volume of LDH reagent into each well, the absorbance was measured using a spectrophotometer at a wavelength of 492 nm with a reference wavelength of 620 nm. For more accurate measurements, the absorbance of the no-cell controls was subtracted from the readings of CM samples.

Flow Cytometry Analyses of Cell Retention in the Hearts after Tissue Digestion. To investigate the effects of PA-RGDS on cell engraftment and cell survival *in vivo*, cultured HL-1 CMs with or without PA-RGDS gel encapsulation were prelabeled with CM-DiI, a red fluorescent dye, and intramyocardially injected into the hearts of uninjured athymic nude mice (5×10^5 cells per mouse) through 30G needles at two sites of myocardium ($N = 3$ per group). After 7 days, the hearts were harvested for further analyses. For quantification of surviving HL-1 CMs, we performed flow cytometry analysis after tissue digestion. The cell-injected areas in each heart were removed, minced, and digested with collagenase type II (50 U/mL; Worthington Biochemicals) at 37 °C for 60−90 min. Single-cell suspensions were prepared by filtering through a 50 μm strainer. Cells were then analyzed by a C6 flow cytometer (BD Biosciences), and flow cytometric data were analyzed with FlowJo software (Treestar).[35]

Immunocytochemistry and Immunohistochemistry. Cells or frozen heart sections prepared with OCT compound (Tissue-TeK 4583, Sakura Finetek Inc.) were fixed with 4% paraformaldehyde for 10 min at room temperature, washed twice with PBS, and permeabilized with 0.1 or 0.5% Triton X-100 in PBS for 10 min or 1 h. Samples were then blocked with 1% BSA in PBS for 60 min at room temperature and incubated with either anti-ACTN2 (Sigma; 1:100), or mouse anti-TNNT2 (NeoMarkers; 1:100), or mouse anti-MYH6/7 (Abcam; 1:100), or Gja1 (Sigma; 1:100) at 4 °C overnight. The samples were again washed three times with PBS containing 1% Tween 20 and then incubated with anti-mouse IgG−Alexa Fluor 594 (Invitrogen; 1:1000) or antimouse IgG−Alexa Fluor 488 (Invotrogen; 1:1000) in PBS for 60 min at room temperature. DAPI was used for nuclear staining. The samples were visualized under a fluorescent microscope (Nikon) or a Zeiss LSM 510 Meta confocal laser scanning microscope and analyzed by LSM 510 Image software (CLSM, Carl Zeiss).

Mouse ESC Culture and Differentiation. mESCs (J1) were cultured in high-glucose Dulbecco's modified Eagle medium (DMEM) supplemented with 10% FBS (Atlanta Biologicals), 1% nonessential amino acids solution, 1% L-glutamine, 0.1 mM β-mercaptoethanol, 1% penicillin/streptomycin, and 2000 U/mL mouse LIF (Millipore) on feeder layers of mitotically inactivated STO cells, a mouse embryonic fibroblast line (ATCC). To differentiate mESCs into cardiac lineage, an embryoid body (EB) method was employed with some modifications.[47] EBs were formed by suspending the cells at 10^7 cells/mL in 10 mL of differentiation media: alpha-modified Eagle medium (α-MEM; Invitrogen) supplemented with 10% FBS, 1% nonessential amino acids, 1% L-glutamine, 1% β-mercaptoethanol, L-ascorbic acid (50 μg/mL; Sigma), and 1% penicillin/streptomycin. Differentiation medium was changed every day. Four days after the initiation of EB formation, floating EBs were collected by centrifugation and transferred to fibronectin (Sigma)-coated plates to be attached. Then these attached EBs on fibronectin-coated plates were cultured in nonserum culture medium: DMEM/F12 (Invitrogen) supplemented with L-ascorbic acid (50 μg/mL) for further differentiation into CMs. Typically, beating cells appeared on day 7.

Enrichment of mESC-Derived Cardiomyocytes Using Lactate. To enrich the CMs from mESC differentiation cultures, lactate-based purification was applied.[36] The cardiomyogenically differentiated mESCs at day 11 were dissociated with trypsin (0.05%), replated in fibronectin-coated dishes containing freshly prepared glucose-free advanced DMEM (no glucose, no pyruvate; Invitrogen) supplemented with 1 mM lactate, 0% FBS, 1% nonessential amino acids, 1% L-glutamine, 1% β-mercaptoethanol, and 1% penicillin/streptomycin, and continuously cultured for 7 days. Medium was changed every 2 days in order to eliminate dead cells. After 7 days of culture in lactase-containing media, the enriched mESC-derived CMs were dissociated with trypsin (0.05%), transferred to fibronectin-coated dishes, and further cultured with α-MEM supplemented with 3% FBS and ITS. To quantify the CMs, flow cytometric analysis following cell permeabilization was performed using ACTN2 antibody (Sigma).[32]

Induction of Myocardial Infarction and Cardiomyocyte Transplantation. All animal experiments were approved by the Emory University Institutional Animal Care and Use Committee and were performed in accordance with federal guidelines. Studies were performed using male athymic nude mice (Foxn1^{nu}) (Harlan, USA). Myocardial infarction and cell implantation were performed as described previously.[48] MI was induced in mice by ligation of the left anterior descending coronary artery, and cells or other reagents were intramyocardially injected through 30 G needles at two different sites in the border zone of the myocardium immediately after surgery. Mice were randomly assigned into four treatment groups: (i) PBS as a control group, (ii) 2×10^5 mESCs-derived CMs only, (iii) PA-RGDS only, or (iv) 2×10^5 mESCs-derived CMs encapsulated with PA-RGDS. Due to the limiting factor of murine heart size and the requirement to deliver a large quantity of cells, only one concentration ratio of PA (2×10^5 mESCs-derived CMs[32]) to cells was used for the studies. All CMs were obtained from the same differentiation batch and prelabeled with CM-DiI (red fluorescence) before cell injection for cell tracking in histology. The number of mice was 10−12 per experimental group.

Echocardiography. Echocardiography was performed at week 1, 2, 4, 8, and 12 after surgery using a Vevo 770TM Imaging System (VisualSonics, Inc.) as previously described.[33] Ejection fraction and fractional shortening were measured using two-dimensional and M-mode images.

Masson's Trichrome Staining and Measurement of Fibrosis. To determine the circumferential fibrosis area, heart tissues were harvested 4 weeks after MI induction and treatments and stained with Masson's trichrome (Sigma-Aldrich) as previously described.[49] Fibrosis and LV areas were measured, and average ratios (fibrosis:LV areas) were calculated.

Statistical Analyses. All data were expressed as mean ± SEM. Student's t test or ANOVA test was used for the statistical analysis. Repeated-measures ANOVA was used for data shown in Figure 6A. Values of $p < 0.05$ were considered to denote statistical significance. All statistical analyses were conducted using SPSS 20.0 (SPSS Inc.).

Conflict of Interest: The authors declare no competing financial interest.

Acknowledgment. This work was supported in part by the NHLBI of the NIH as a Program of Excellence in Nanotechnology award (HHSN268201000043C), by grants from NIDDK (DP3DK094346), and the National Science Foundation STC award (CBET-0939511). K.B. is a recipient of an American Heart Association postdoctoral fellowship grant.

Supporting Information Available: Supplementary Figure 1: Degradation of PA-RGDS *in vivo*. Supplementary Figure 2: Generation of enriched cardiomyocytes from differentiating mESCs. Supplementary Movie 1: Contraction of mESC-derived cardiomyocytes. This material is available free of charge *via* the Internet at http://pubs.acs.org.

REFERENCES AND NOTES

1. Members, W. G.; Roger, V. L.; Go, A. S.; Lloyd-Jones, D. M.; Benjamin, E. J.; Berry, J. D.; Borden, W. B.; Bravata, D. M.; Dai, S.; Ford, E. S.; *et al.* Heart Disease and Stroke Statistics—2012 Update. *Circulation* **2012**, *125*, e2–e220.
2. Laflamme, M. A.; Murry, C. E. Heart Regeneration. *Nature* **2011**, *473*, 326–335.
3. Takahashi, K.; Tanabe, K.; Ohnuki, M.; Narita, M.; Ichisaka, T.; Tomoda, K.; Yamanaka, S. Induction of Pluripotent Stem Cells from Adult Human Fibroblasts by Defined Factors. *Cell* **2007**, *131*, 861–872.
4. Park, I.-H.; Arora, N.; Huo, H.; Maherali, N.; Ahfeldt, T.; Shimamura, A.; Lensch, M. W.; Cowan, C.; Hochedlinger, K.; Daley, G. Q. Disease-Specific Induced Pluripotent Stem Cells. *Cell* **2008**, *134*, 877–886.
5. Zwi, L.; Caspi, O.; Arbel, G.; Huber, I.; Gepstein, A.; Park, I. H.; Gepstein, L. Cardiomyocyte Differentiation of Human Induced Pluripotent Stem Cells. *Circulation* **2009**, *120*, 1513–1523.
6. Kattman, S. J.; Witty, A. D.; Gagliardi, M.; Dubois, N. C.; Niapour, M.; Hotta, A.; Ellis, J.; Keller, G. Stage-Specific Optimization of Activin/Nodal and Bmp Signaling Promotes Cardiac Differentiation of Mouse and Human Pluripotent Stem Cell Lines. *Cell Stem Cell* **2011**, *8*, 228–240.
7. Burridge, P. W.; Keller, G.; Gold, J. D.; Wu, J. C. Production of de Novo Cardiomyocytes: Human Pluripotent Stem Cell Differentiation and Direct Reprogramming. *Cell Stem Cell* **2012**, *10*, 16–28.
8. Mignone, J. L.; Kreutziger, K. L.; Paige, S. L.; Murry, C. E. Cardiogenesis from Human Embryonic Stem Cells—Mechanisms and Applications. *Circ. J.* **2010**, *74*, 2517–2526.
9. Mummery, C.; Ward-van Oostwaard, D.; Doevendans, P.; Spijker, R.; van den Brink, S.; Hassink, R.; van der Heyden, M.; Opthof, T.; Pera, M.; de la Riviere, A. B.; *et al.* Differentiation of Human Embryonic Stem Cells to Cardiomyocytes: Role of Coculture with Visceral Endoderm-Like Cells. *Circulation* **2003**, *107*, 2733–2740.
10. Zhang, M.; Methot, D.; Poppa, V.; Fujio, Y.; Walsh, K.; Murry, C. E. Cardiomyocyte Grafting for Cardiac Repair: Graft Cell Death and Anti-Death Strategies. *J. Mol. Cell. Cardiol.* **2001**, *33*, 907–921.
11. van Laake, L. W.; Passier, R.; Doevendans, P. A.; Mummery, C. L. Human Embryonic Stem Cell—Derived Cardiomyocytes and Cardiac Repair in Rodents. *Circ. Res.* **2008**, *102*, 1008–1010.
12. Segers, V. F. M.; Lee, R. T. Biomaterials to Enhance Stem Cell Function in the Heart. *Circ. Res.* **2011**, *109*, 910–922.
13. Hartgerink, J. D.; Beniash, E.; Stupp, S. I. Self-Assembly and Mineralization of Peptide-Amphiphile Nanofibers. *Science* **2001**, *294*, 1684–1688.
14. Jun, H. W.; Yuwono, V.; Paramonov, S. E.; Hartgerink, J. D. Enzyme Meidated Degradation of Peptide-Amphiphile Nanofiber Networks. *Adv. Mater.* **2005**, *17*, 2612–2617.
15. Benton, J. A.; Fairbanks, B. D.; Anseth, K. S. Characterization of Valvular Interstitial Cell Function in Three Dimensional Matrix Metalloproteinase Degradable Peg Hydrogels. *Biomaterials* **2009**, *30*, 6593–6603.
16. Yu, J.; Gu, Y.; Du, K. T.; Mihardja, S.; Sievers, R. E.; Lee, R. J. The Effect of Injected Rgd Modified Alginate on Angiogenesis and Left Ventricular Function in a Chronic Rat Infarct Model. *Biomaterials* **2009**, *30*, 751–756.
17. Yu, J.; Du, K. T.; Fang, Q.; Gu, Y.; Mihardja, S. S.; Sievers, R. E.; Wu, J. C.; Lee, R. J. The Use of Human Mesenchymal Stem Cells Encapsulated in Rgd Modified Alginate Microspheres in the Repair of Myocardial Infarction in the Rat. *Biomaterials* **2010**, *31*, 7012–7020.
18. Mihardja, S. S.; Gonzales, J. A.; Gao, D.; Sievers, R. E.; Fang, Q.; Stillson, C. A.; Yu, J.; Peng, M.; Lee, R. J. The Effect of a Peptide-Modified Thermo-Reversible Methylcellulose on Wound Healing and Lv Function in a Chronic Myocardial Infarction Rodent Model. *Biomaterials* **2013**, *34*, 8869–8877.
19. Gandaglia, A.; Huerta-Cantillo, R.; Comisso, M.; Danesin, R.; Ghezzo, F.; Naso, F.; Gastaldello, A.; Schittullo, E.; Buratto, E.; Spina, M.; *et al.* Cardiomyocytes *in Vitro* Adhesion Is Actively Influenced by Biomimetic Synthetic Peptides for Cardiac Tissue Engineering. *Tissue Eng. Part A* **2012**, *18*, 725–736.
20. Sapir, Y.; Kryukov, O.; Cohen, S. Integration of Multiple Cell-Matrix Interactions into Alginate Scaffolds for Promoting Cardiac Tissue Regeneration. *Biomaterials* **2011**, *32*, 1838–1847.
21. Shachar, M.; Tsur-Gang, O.; Dvir, T.; Leor, J.; Cohen, S. The Effect of Immobilized Rgd Peptide in Alginate Scaffolds on Cardiac Tissue Engineering. *Acta Biomater.* **2011**, *7*, 152–162.
22. Wang, X.; Cooper, S. Adhesion of Endothelial Cells and Endothelial Progenitor Cells on Peptide-Linked Polymers in Shear Flow. *Tissue Eng. Part A* **2013**, *19*, 1113–1121.
23. Anderson, J. M.; Kushwaha, M.; Tambralli, A.; Bellis, S. L.; Camata, R. P.; Jun, H. W. Osteogenic Differentiation of Human Mesenchymal Stem Cells Directed by Extracellular Matrix-Mimicking Ligands in a Biomimetic Self-Assembled Peptide Amphiphile Nanomatrix. *Biomacromolecules* **2009**, *10*, 2935–2944.
24. Anderson, J. M.; Patterson, J. L.; Vines, J. B.; Javed, A.; Gilbert, S. R.; Jun, H. W. Biphasic Peptide Amphiphile Nanomatrix Embedded with Hydroxyapatite Nanoparticles for Stimulated Osteoinductive Response. *ACS Nano* **2011**, *5*, 9463–9479.
25. Anderson, J. M.; Vines, J. B.; Patterson, J. L.; Chen, H.; Javed, A.; Jun, H. W. Osteogenic Differentiation of Human Mesenchymal Stem Cells Synergistically Enhanced by Biomimetic Peptide Amphiphiles Combined with Conditioned Medium. *Acta Biomater.* **2011**, *7*, 675–682.
26. Vines, J. B.; Lim, D. J.; Anderson, J. M.; Jun, H. W. Hydroxyapatite Nanoparticle Reinforced Peptide Amphiphile Nanomatrix Enhances the Osteogenic Differentiation of Mesenchymal Stem Cells by Compositional Ratios. *Acta Biomater.* **2012**, *8*, 4053–4063.
27. Lim, D. J.; Antipenko, S. V.; Anderson, J. M.; Jaimes, K. F.; Viera, L.; Stephen, B. R.; Bryant, S. M.; Yancey, B. D.; Hughes, K. J.; Cui, W.; *et al.* Enhanced Rat Islet Function and Survival *in Vitro* Using a Biomimetic Self-Assembled Nanomatrix Gel. *Tissue Eng. Part A* **2011**, *17*, 399–406.
28. Lim, D. J.; Antipenko, S. V.; Vines, J. B.; Andukuri, A.; Hwang, P. T.; Hadley, N. T.; Rahman, S. M.; Corbett, J. A.; Jun, H. W. Improved Min6 Beta-Cell Function on Self-Assembled Peptide Amphiphile Nanomatrix Inscribed with Extracellular Matrix-Derived Cell Adhesive Ligands. *Macromol. Biosci.* **2013**, *13*, 1404–1412.
29. Cheung, P.-Y.; Sawicki, G.; Wozniak, M.; Wang, W.; Radomski, M. W.; Schulz, R. Matrix Metalloproteinase-2 Contributes to Ischemia-Reperfusion Injury in the Heart. *Circulation* **2000**, *101*, 1833–1839.
30. Bendeck, M. P.; Zempo, N.; Clowes, A. W.; Galardy, R. E.; Reidy, M. A. Smooth Muscle Cell Migration and Matrix Metalloproteinase Expression after Arterial Injury in the Rat. *Circ. Res.* **1994**, *75*, 539–545.
31. Spinale, F. G.; Coker, M. L.; Thomas, C. V.; Walker, J. D.; Mukherjee, R.; Hebbar, L. Time-Dependent Changes in Matrix Metalloproteinase Activity and Expression During the Progression of Congestive Heart Failure: Relation to Ventricular and Myocyte Function. *Circ. Res.* **1998**, *82*, 482–495.
32. Ban, K.; Wile, B.; Kim, S.; Park, H.-J.; Byun, J.; Cho, K.-W.; Saafir, T.; Song, M.-K.; Yu, S. P.; Wagner, M.; *et al.* Purification of Cardiomyocytes from Differentiating Pluripotent Stem Cells Using Molecular Beacons That Target Cardiomyocyte-Specific Mrna. *Circulation* **2013**, *128*, 1897–1909.
33. Cho, H.-J.; Lee, N.; Lee, J. Y.; Choi, Y. J.; Ii, M.; Wecker, A.; Jeong, J.-O.; Curry, C.; Qin, G.; Yoon, Y.-s. Role of Host Tissues for Sustained Humoral Effects after Endothelial Progenitor Cell Transplantation into the Ischemic Heart. *J. Exp. Med.* **2007**, *204*, 3257–3269.
34. Claycomb, W. C.; Lanson, N. A.; Stallworth, B. S.; Egeland, D. B.; Delcarpio, J. B.; Bahinski, A.; Izzo, N. J. Hl-1 Cells: A Cardiac Muscle Cell Line That Contracts and Retains Phenotypic Characteristics of the Adult Cardiomyocyte. *Proc. Natl. Acad. Sci. U.S.A.* **1998**, *95*, 2979–2984.

35. Kim, H.; Cho, H.-J.; Kim, S.-W.; Liu, B.; Choi, Y. J.; Lee, J.; Sohn, Y.-D.; Lee, M.-Y.; Houge, M. A.; Yoon, Y.-s. Cd31+ Cells Represent Highly Angiogenic and Vasculogenic Cells in Bone Marrow: Novel Role of Nonendothelial Cd31+ Cells in Neovascularization and Their Therapeutic Effects on Ischemic Vascular Disease. *Circ. Res.* **2010**, *107*, 602–614.
36. Tohyama, S.; Hattori, F.; Sano, M.; Hishiki, T.; Nagahata, Y.; Matsuura, T.; Hashimoto, H.; Suzuki, T.; Yamashita, H.; Satoh, Y.; *et al*. Distinct Metabolic Flow Enables Large-Scale Purification of Mouse and Human Pluripotent Stem Cell-Derived Cardiomyocytes. *Cell Stem Cell* **2013**, *12*, 127–137.
37. Lam, M. T.; Wu, Joseph C. Biomaterial Applications in Cardiovascular Tissue Repair and Regeneration. *Expert Rev. Cardiovasc. Ther.* **2012**, *10*, 1039–1049.
38. Vunjak-Novakovic, G.; Lui, K. O.; Tandon, N.; Chien, K. R. Bioengineering Heart Muscle: A Paradigm for Regenerative Medicine. *Annu. Rev. Biomed. Eng.* **2011**, *13*, 245–267.
39. Hsieh, P. C.; Davis, M. E.; Gannon, J.; MacGillivray, C.; Lee, R. T. Controlled Delivery of Pdgf-Bb for Myocardial Protection Using Injectable Self-Assembling Peptide Nanofibers. *J. Clin. Invest.* **2006**, *116*, 237–248.
40. Frederick, J. R.; Fitzpatrick, J. R.; McCormick, R. C.; Harris, D. A.; Kim, A.-Y.; Muenzer, J. R.; Marotta, N.; Smith, M. J.; Cohen, J. E.; Hiesinger, W.; *et al*. Stromal Cell-Derived Factor-1α Activation of Tissue-Engineered Endothelial Progenitor Cell Matrix Enhances Ventricular Function after Myocardial Infarction by Inducing Neovasculogenesis. *Circulation* **2010**, *122*, S107–S117.
41. Lin, Y.-D.; Yeh, M.-L.; Yang, Y.-J.; Tsai, D.-C.; Chu, T.-Y.; Shih, Y.-Y.; Chang, M.-Y.; Liu, Y.-W.; Tang, A. C. L.; Chen, T.-Y.; *et al*. Intramyocardial Peptide Nanofiber Injection Improves Postinfarction Ventricular Remodeling and Efficacy of Bone Marrow Cell Therapy in Pigs. *Circulation* **2010**, *122*, S132–S141.
42. Gnecchi, M.; Zhang, Z.; Ni, A.; Dzau, V. J. Paracrine Mechanisms in Adult Stem Cell Signaling and Therapy. *Circ. Res.* **2008**, *103*, 1204–1219.
43. Anderson, J. M.; Andukuri, A.; Lim, D. J.; Jun, H. W. Modulating the Gelation Properties of Self-Assembling Peptide Amphiphiles. *ACS Nano* **2009**, *3*, 3447–3454.
44. Andukuri, A.; Minor, W. P.; Kushwaha, M.; Anderson, J. M.; Jun, H. W. Effect of Endothelium Mimicking Self-Assembled Nanomatrices on Cell Adhesion and Spreading of Human Endothelial Cells and Smooth Muscle Cells. *Nanomed.: Nanotechnol., Biol., Med.* **2010**, *6*, 289–297.
45. Andukuri, A.; Sohn, Y. D.; Anakwenze, C. P.; Lim, D. J.; Brott, B. C.; Yoon, Y. S.; Jun, H. W. Enhanced Human Endothelial Progenitor Cell Adhesion and Differentiation by a Bioinspired Multifunctional Nanomatrix. *Tissue Eng. Part C* **2013**, *19*, 375–385.
46. Ban, K.; Kim, K.-H.; Cho, C.-K.; Sauvé, M.; Diamandis, E. P.; Backx, P. H.; Drucker, D. J.; Husain, M. Glucagon-Like Peptide (Glp)-1(9−36)Amide-Mediated Cytoprotection Is Blocked by Exendin(9−39) Yet Does Not Require the Known Glp-1 Receptor. *Endocrinology* **2010**, *151*, 1520–1531.
47. Hescheler, J.; Fleischmann, B. K.; Lentini, S.; Maltsev, V. A.; Rohwedel, J.; Wobus, A. M.; Addicks, K. Embryonic Stem Cells: A Model to Study Structural and Functional Properties in Cardiomyogenesis. *Cardiovasc. Res.* **1997**, *36*, 149–162.
48. Jeong, J.-O.; Han, J. W.; Kim, J.-M.; Cho, H.-J.; Park, C.; Lee, N.; Kim, D.-W.; Yoon, Y.-S. Malignant Tumor Formation after Transplantation of Short-Term Cultured Bone Marrow Mesenchymal Stem Cells in Experimental Myocardial Infarction and Diabetic Neuropathy. *Circ. Res.* **2011**, *108*, 1340–1347.
49. Yoon, Y.-s.; Wecker, A.; Heyd, L.; Park, J.-S.; Tkebuchava, T.; Kusano, K.; Hanley, A.; Scadova, H.; Qin, G.; Cha, D.-H.; *et al*. Clonally Expanded Novel Multipotent Stem Cells from Human Bone Marrow Regenerate Myocardium after Myocardial Infarction. *J. Clin. Invest* **2005**, *115*, 326–338.